Tohoku J. Exp. Med., 2025, **266**, 1-9

Identification of Two Subtypes with Distinct Immune Features in Lung Adenocarcinoma by Utilizing Immune and Metabolism-Related Genes to Assist Immunotherapy

Mengna Wang[1] and Hongbo Xia[1]

[1]Department of Respiratory Medicine, Affiliated Xiaoshan Hospital, Hangzhou Normal University, Hangzhou, China

This work was designed to explore the value of immune and metabolism-related genes (IMRGs) in lung adenocarcinoma (LUAD) prognosis, with the intention of aiding the application of immunotherapy in LUAD patients. Differential gene expression analysis was conducted using The Cancer Genome Atlas (TCGA)-LUAD data. After merging and deduplication, an intersection was taken with LUAD differential genes to acquire IMRGs. 716 IMRGs were utilized for LUAD clustering, resulting in the stratification of LUAD patients into two subtypes. Cluster-1 demonstrated higher immunophenoscore and lower tumor immune dysfunction and exclusion scores, indicating that cancer patients in cluster-1 were more likely to benefit from immune checkpoint inhibitor therapy. Somatic mutation analysis revealed higher mutation rates in both sample and gene levels for cluster-2 compared to cluster-1. Additionally, we predicted ten prospective candidate drugs, including Teniposide and phloretin, for LUAD patients. LUAD was stratified into two subtypes with distinct molecular features based on IMRGs. These subtypes exhibited pronounced differences in immune processes, checkpoints, genetic mutations, and drug sensitivity. Our endeavor has furnished invaluable insights into comprehending the molecular characteristics of LUAD, potentially enhancing the precision of immunotherapeutic strategies tailored for LUAD.

Keywords: immune-related genes; lung adenocarcinoma; metabolism-related genes; molecular features; prognosis
Tohoku J. Exp. Med., 2025 May, **266** (1), 1-9.
doi: 10.1620/tjem.2024.J086

Introduction

Lung cancer (LC), distinguished by its elevated incidence and mortality rates, persists as a malignancy of worldwide significance. According to the 2020 Global Cancer Statistics report, approximately 2.2 million new cases of LC were estimated worldwide, accounting for the second highest incidence (11.4%), and 1.8 million new deaths were reported, making it the leading cause of cancer-related mortality (18.0%) (Sung et al. 2021). Among its subtypes, lung adenocarcinoma (LUAD) stands as a predominant variant (Nooreldeen and Bach 2021). LUAD is marked by its extended latency period, subtle early symptoms, and high malignancy. Furthermore, a considerable proportion of cases involving LUAD are identified at an advanced stage, thus bypassing the most opportune phase for therapeutic intervention (Blandin Knight et al. 2017). Despite significant breakthroughs in clinical diagnosis and treatment strategies, such as targeted therapies and immunotherapies (Cancer Genome Atlas Research Network 2014), LUAD patients still grapple with challenges including postoperative recurrence, low drug sensitivity, and unfavorable prognosis (Seguin et al. 2022). Consequently, an immediate imperative exists to enhance both diagnostic and therapeutic benchmarks for LUAD. Conventional pathological staging often dictates treatment decisions; however, the heterogeneous nature of LUAD in radiology, pathology, and molecular domains underscores the current lack of multidisciplinary integration (Socinski et al. 2016). With the advent of sequencing technologies, LUAD research and treatment paradigms have evolved from pure histopathological subtyping to molecular classification (Kashima et al. 2019). Throughout LUAD's initiation and progression, distinct driver gene mutations interact to medi-

Received April 15, 2024; revised and accepted August 25, 2024; J-STAGE Advance online publication September 5, 2024
Correspondence: Hongbo Xia, Department of Respiratory Medicine, Affiliated Xiaoshan Hospital, Hangzhou Normal University, No.728, Yucai North Road, Chengxiang Town, Xiaoshan District, Hangzhou City, Zhejiang Province 311200, China.
e-mail: hongbxia@163.com

ate tumor evolution, evident in the spectrum of tumor heterogeneity (Inamura 2018). Thus, an analysis amalgamating molecular classification and clinical-pathological features of LUAD holds promise for optimizing personalized treatments for patients.

Immunoreactivity (Liu et al. 2022) and metabolic reprogramming (Martínez-Reyes and Chandel 2021) play pivotal roles in tumor initiation and progression. There exists a robust interplay between cellular immunity and metabolic reprogramming (Li et al. 2019). Metabolic processes not only provide the essential energy required for immune cell activity (Xia et al. 2021) but also contribute to immune suppression and tumor promotion within the tumor microenvironment (TME) (Bader et al. 2020). Thus, a classification of LUAD based on either immunological or metabolic perspectives can unveil distinct molecular features. Utilizing RNA sequencing profiles of LUAD from The Cancer Genome Atlas (TCGA) and Gene Expression Omnibus (GEO) databases encompassing genes associated with immune activation, Zeng et al. (2023) segregated patients into two clusters, exhibiting differential survival and immune cell infiltration. Huang et al. (2023), using metabolism-associated genes from TCGA and GEO data, categorized LUAD patients into three molecular clusters, revealing varying prognosis, metabolic pathways, immune processes, and checkpoints. Choi and Na (2018), relying on the characteristics of TME glycolysis and immune cell infiltration in LUAD transcriptome data, divided patients into four clusters showcasing distinct immune cell composition, tumor metabolism, and survival. In this endeavor, we amalgamated immune and metabolism-related genes (IMRGs) gleaned from prior studies and integrated them with LUAD samples for molecular subtyping.

As depicted in Fig. 1, we leveraged the dataset from TCGA database to perform molecular subtyping of LUAD samples ground on IMRGs. Subsequently, we evaluated the inter-class survival outcomes, immune cell infiltration, immunotherapy response, protein-protein interaction (PPI) networks and enrichment analysis, somatic mutations, and prediction of targeted small molecules. This study endeavored to enhance the prognosis and treatment strategies for LUAD.

Materials and Methods

Data source

RNA sequencing transcriptomic data of LUAD were obtained from TCGA database (https://portal.gdc.cancer.gov/), comprising 59 normal samples and 541 LUAD samples. The patients included were mainly pathologically diagnosed with LUAD and had no other comorbidities. Metabolism-related genes (MRGs) (Cui et al. 2023) and immune-related genes (IRGs) (Bhattacharya et al. 2014) were sourced from both literature and the ImmPort database (https://immport.niaid.nih.gov).

Differential expression analysis

The R package edgeR was employed to analyze differentially expressed genes (DEGs) within LUAD and Normal samples (Robinson et al. 2010). DEGs were selected using criteria FDR < 0.05 and |log(FC)| >1. After integration and

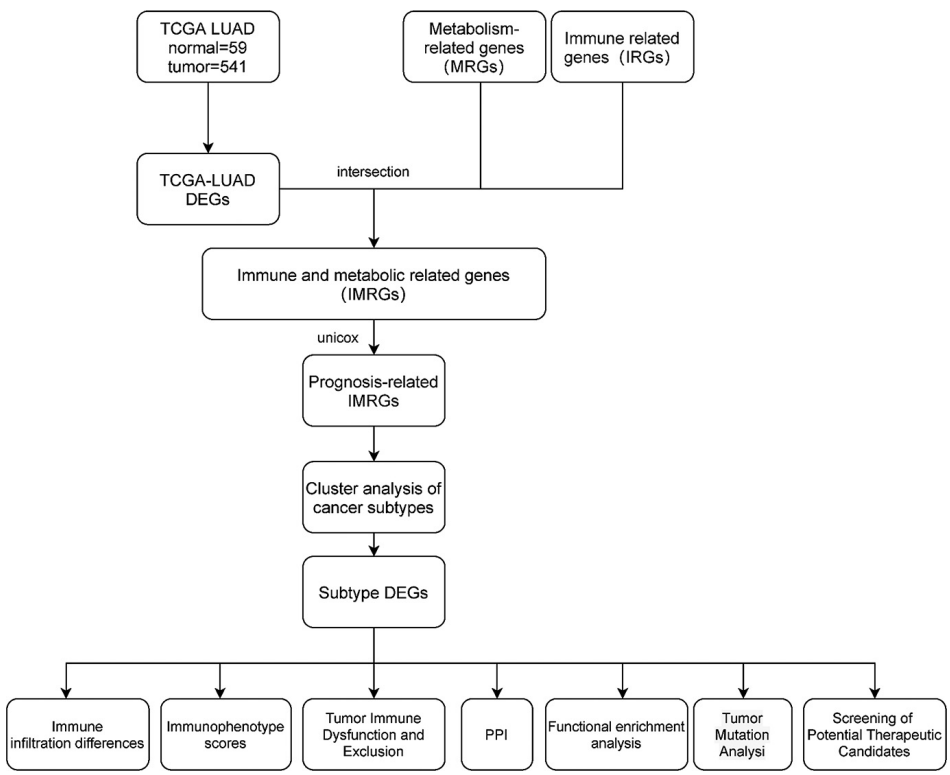

Fig. 1. Workflow diagram.

deduplication of MRGs and IRGs, intersection was taken with DEGs, obtaining differential IMRGs.

Unsupervised consensus clustering of IMRGs

IMRGs associated with LUAD prognosis were identified using univariate Cox regression analysis. R package ConsensusClusterPlus was used to conduct 1,000 repetitions of consensus clustering analysis to ensure stability and optimal cluster numbers (Wilkerson and Hayes 2010). The survival R package was utilized to investigate survival differences among clusters.

Immune infiltration and immune factor analysis between different molecular subtypes

R packages Estimation of STromal and Immune cells in MAlignant Tumor tissues using Expression data (ESTIMATE) (Yoshihara et al. 2013), Cell-type Identification by Estimating Relative Subsets of RNA Transcripts (CIBERSORT) (Newman et al. 2015), and gene set variation analysis (GSVA) (Hänzelmann et al. 2013) were respectively employed for immune infiltration and immune factor analysis. Visualization was performed using the R package pheatmap. Further assessment was conducted to evaluate the expression patterns of human leukocyte antigen (HLA) and immune checkpoint-related genes within the two subtypes.

Analysis of immunophenoscore (IPS) and tumor immune dysfunction and exclusion (TIDE) score between different molecular subtypes

IPS and TIDE scores were analyzed using The Cancer Immunome Atlas (TCIA, https://tcia.at) and TIDE (harvard.edu) databases to uncover differences between the two subtypes.

PPI network and Gene Ontology (GO)/Kyoto Encyclopedia of Genes and Genomes (KEGG) analysis of DEGs between different molecular subtypes

The R package edgeR was used to analyze DEGs (FDR < 0.05 & |log (FC)| > 1) between the two subtype samples. The STRING database (https://cn.string-db.org/) was used to construct a PPI network for DEGs (highest confidence > 0.7). R package ClusterProfiler (Yu et al. 2012) was used to conduct GO enrichment and KEGG pathway analyses on DEGs to illuminate potential functional pathways. Results were visualized using the R package enrichplot.

Tumor mutation analysis of different molecular subtypes

Mutation data for single nucleotide variants (SNVs) of LUAD patients were obtained. The R package maftools (Mayakonda et al. 2018) was utilized to analyze and visualize mutation status, mutation types, SNV classes, and mutation rates differences between the two subtypes, and the top ten genes with the highest mutation rates within the two subtypes were screened.

Analysis of targeted small molecules for LUAD

The Connectivity Map (cMAP) database (https://clue.io/) enables comparison of drugs highly correlated with tumors using gene expression profile data, inferring the principal structure of most drug molecules, and deducing potential mechanisms of action (Yang et al. 2013). Through the cMAP database, the top 150 DEGs of the two subtypes were used to predict targeted small molecules for LUAD.

Statistical analysis

For bioinformatics data, the entire dataset was filtered by removing missing and duplicate data, and all statistical analysis and visualization was performed using R software (version 3.6.3) (http://www.rproject.org/). Survival analysis was performed using Kaplan-Meier method and log-rank test. Univariate Cox regression analysis was used to evaluate prognostic IMRGs. ConsensusCluster Plus R package was used to perform consensus cluster analysis and 1,000 repetitions to ensure classification stability and optimal cluster number. $P < 0.05$ was considered statistically significant.

Results

LUAD molecular subtypes based on IMRGs

Expression data of LUAD were downloaded from TCGA database. Differential analysis between LUAD and normal samples yielded 5,576 DEGs. A total of 619 MRGs were sourced from the literature (Supplementary Table S1), and 2,483 IRGs were obtained from the ImmPort database (Supplementary Table S2). After integration, deduplication, and intersection with DEGs, 716 IMRGs were identified (Fig. 2A and Supplementary Table S3). Univariate Cox regression analysis identified 169 IMRGs correlated with prognosis (Supplementary Table S4). Based on the expression profiles of these genes, consensus clustering was applied to classify patients, determining the optimal number of clusters as 2 (Fig. 2B,C). This led to the identification of two distinct molecular subtypes, denoted as cluster-1 and cluster-2 (Fig. 2D), containing 265 and 215 patient samples respectively (Supplementary Table S5). Further survival analysis revealed that cluster-1 exhibited a higher overall survival rate (Fig. 2E), implying that patients within cluster-1, under the IMRG expression pattern, might experience a more favorable prognosis and survival outcome.

Analysis of immune features between molecular subtypes

Immune infiltration profoundly influences clinical treatment and features in tumor development. To mine immune features between the two molecular subtypes, we employed ESTIMATE R package to score stromal and immune cells in LUAD tumor samples from the TCGA dataset. The results indicated significantly higher stromal, immune, and ESTIMATE scores in cluster-1 compared to cluster-2 (Fig. 3A). Subsequently, we utilized CIBERSORT and single sample gene set enrichment analysis (ssGSEA) to further investigate differences in immune levels between

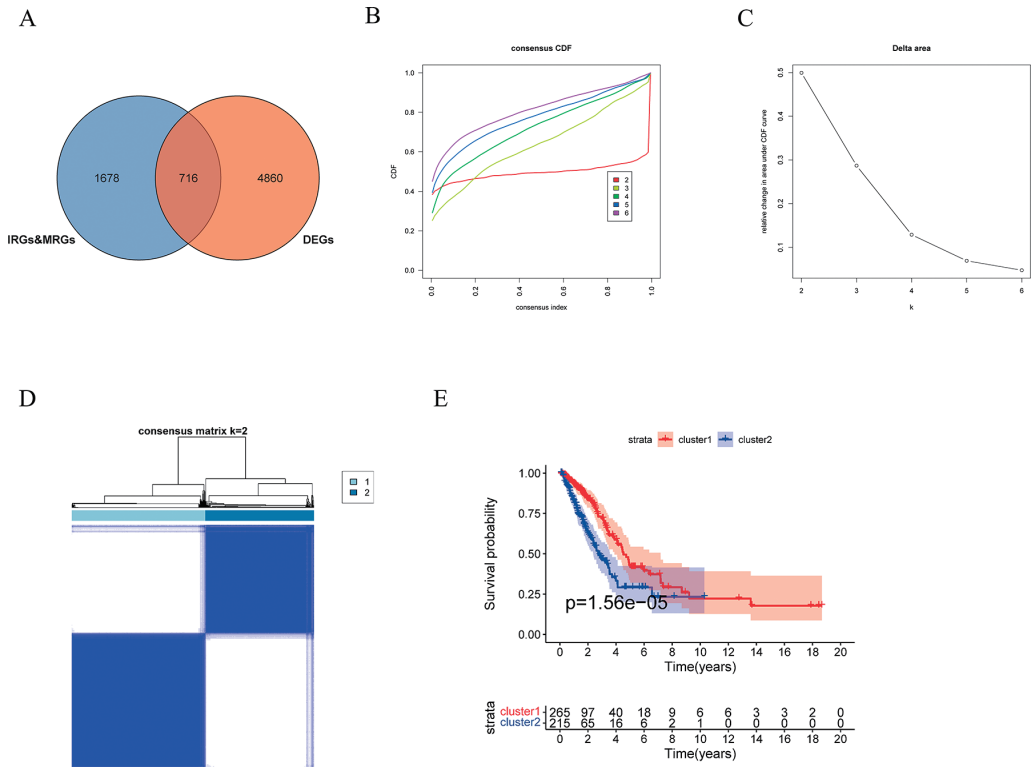

Fig. 2. Molecular subtyping based on IMRGs.
(A) Integration and intersection of IRGs with DEGs; (B) Cumulative distribution function (CDF) curve of TCGA cohort samples; (C) CDF delta area curve of TCGA cohort samples indicating relative changes in the cumulative distribution function area for each category number (k) compared to K-1; (D) Heatmap of TCGA cohort sample clustering; (E) Kaplan-Meier (KM) survival curves for overall survival (OS) prognosis of the two subtypes in the TCGA cohort.

the two subtypes. CIBERSORT analysis revealed higher infiltration levels of B cell memory, T cells CD4 memory resting, Monocytes, Macrophages M2, Dendritic cells resting, Dendritic cells activated, and Mast cells resting in cluster-1. Conversely, cluster-2 exhibited enrichment in Plasma cells, T cells CD4 memory activated, NK cells resting, Macrophages M0, Macrophages M1, and Mast cells activated (Fig. 3B). Through ssGSEA analysis, we explored the distinct distribution of 16 immune infiltrating cells between the two risk groups, with results demonstrating higher abundance of aDCs, B cells, DCs, iDCs, Macrophages, Mast cells, Neutrophils, pDCs, T helper cells, TIL, and Treg cells in cluster-1, with a more noticeable elevation of Th2_cells in cluster-2 (Fig. 3C,D). Cluster-1 exhibited higher immune scores in APC co-inhibition/stimulation, Chemokine receptors (CCR), Checkpoint, HLA, Parainflammation, type_I_IFN Response, and type_II_IFN Response (Fig. 3C,E), suggesting stronger and more active immune responses in cluster-1 associated with better prognosis. Crucial in cancer immunology as molecules responsible for antigen presentation to T lymphocytes, expression of HLA genes between the two subtypes was explored. With the exception of HLA-A, other HLA genes showed higher expression in cluster-1 (Fig. 3F). ICs and their ligands are potential therapeutic targets. Further analysis of the expression of 12 immune checkpoint inhibitors (ICIs) revealed higher expressions of CD28, ICOS, BTLA, CD27, CD40LG, and CD96 in cluster-1, while LAG3 and CEACAM19 were more expressed in cluster-2 (Fig. 3G). In summary, this combined immune and metabolic grouping could serve as a potential biomarker for ICI therapy.

Immunotherapy assessment between molecular subtypes

To study the differences in immunotherapy outcomes between distinct immune and metabolic molecular subtypes, we obtained IPS scores of LUAD from TCIA (Supplementary Table S6). We plotted the IPS score differences between the two subtypes within LUAD-TCGA cancer samples (Fig. 4A). The results indicated significantly higher IPS scores in cluster-1 compared to cluster-2, implying that cancer patients in cluster-1 might benefit more from ICI therapy. Further computation of the TIDE score was performed to predict the level of immune escape in immunotherapy (Supplementary Table S7). Fig. 4B showed that cluster-1 had lower TIDE scores than cluster-2, suggesting a lower likelihood of immune evasion for patients in cluster-1. Therefore, cluster-1 patients were more predisposed to benefit from ICI therapy.

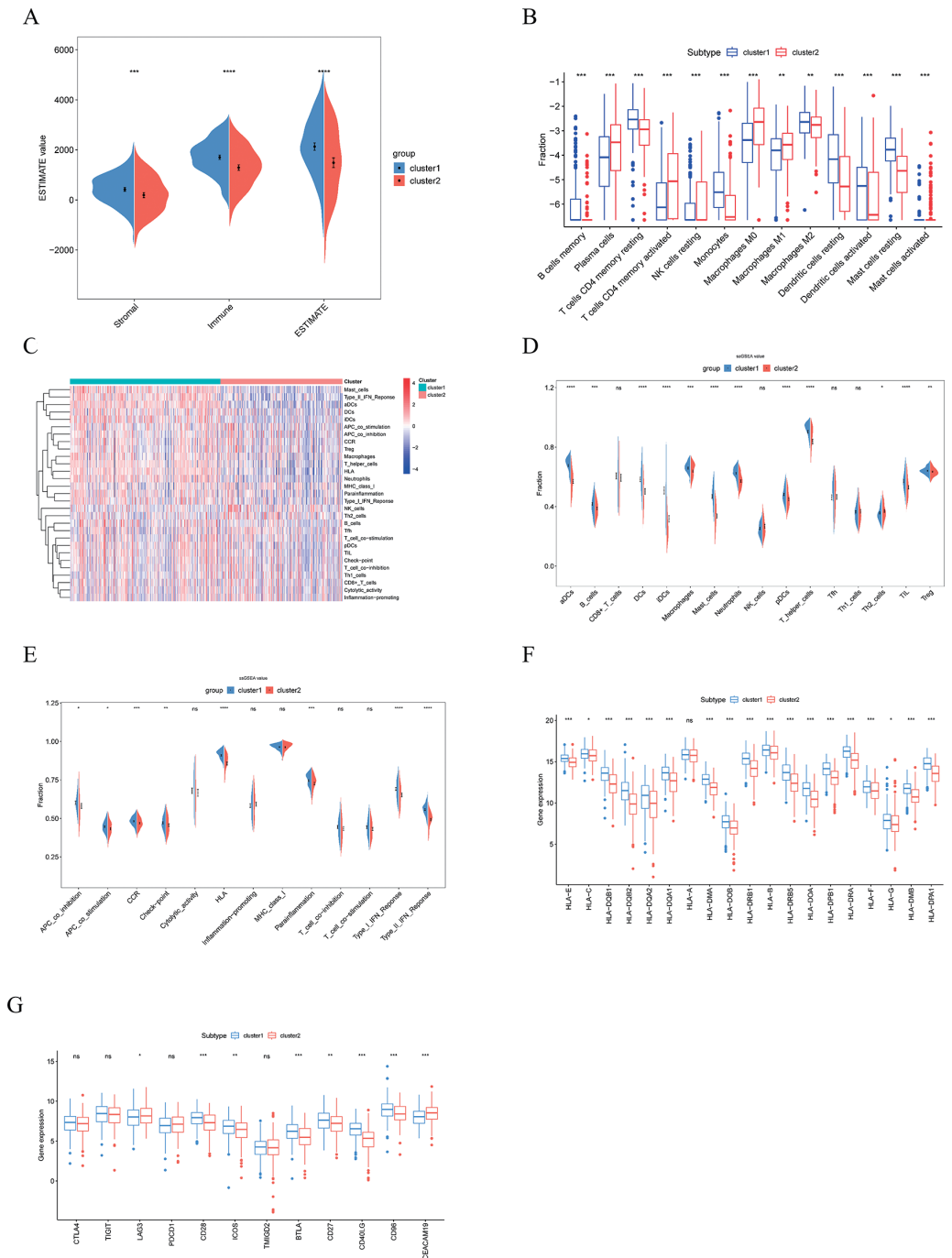

Fig. 3. Assessment of immune infiltration between molecular subtypes.
(A) Differential analysis of ESTIMATE immune-related scores between the two subtypes; (B) Differential analysis of CIBERSORT immune cell components between the two subtypes; (C) Heatmap of ssGSEA analysis for immune cell components in the two subtypes; (D) Differential analysis of immune cell components in the two subtypes using ssGSEA; (E) Differential analysis of immune functional components in the two subtypes using ssGSEA; (F) Analysis of HLA expression between the two subtypes; (G) Analysis of immune checkpoint expression between the two subtypes; * indicates $P < 0.05$, ** indicates $P < 0.01$, *** indicates $P < 0.001$, NS indicates $P > 0.05$.

PPI network construction and GO/KEGG enrichment analysis between molecular subtypes

To uncover the potential biological significance of DEGs within IMRGs subtypes, we performed DEG analysis between cluster-1 and cluster-2, resulting in 2,197 DEGs (Supplementary Table S8). Subsequently, we constructed a PPI network for these DEGs, which consisted of 1,001 nodes and 374 edges (Fig. 5A). Functional exploration of DEGs in the two subtypes was carried out through GO and KEGG enrichment analyses. GO enrichment showed that DEGs were enriched in functions such as channel activity, passive transmembrane transporter activity, and collagen-

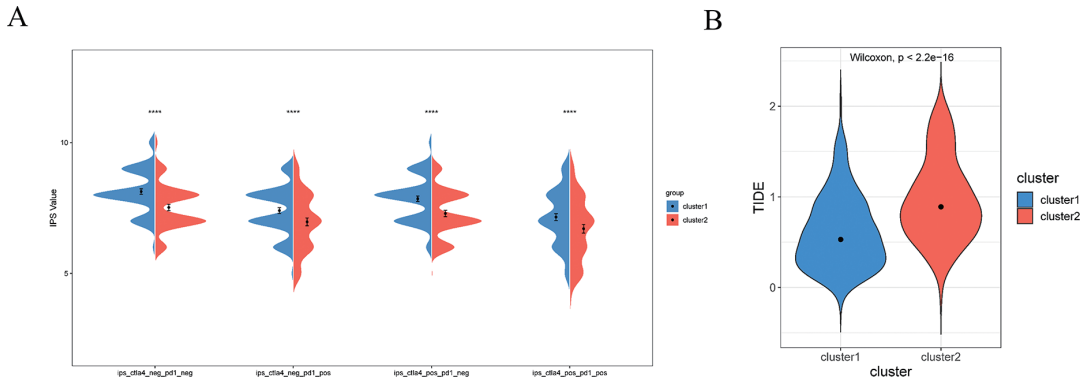

Fig. 4. Assessment of immunotherapy in molecular subtypes.
(A) IPS scores of the two subtypes; (B) TIDE scores of the two subtypes; *** indicates $P < 0.001$.

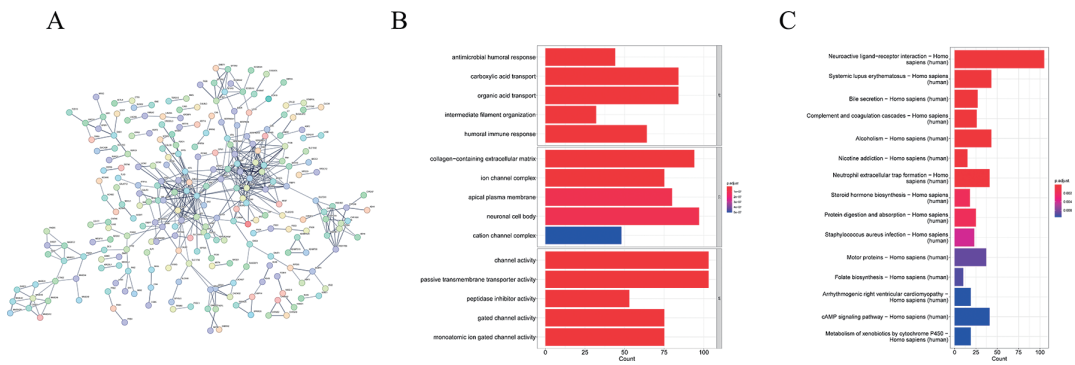

Fig. 5. PPI construction and GO/KEGG enrichment analysis.
(A-C) PPI network diagram (A), GO enrichment analysis results (B), and KEGG enrichment analysis results (C) of DEGs in the two clusters. BP, biological process; CC, cellular component; MF, molecular function.

containing extracellular matrix (Fig. 5B). KEGG analysis revealed that DEGs were enriched in pathways like Neuroactive ligand-receptor interaction, Systemic lupus erythematosus, and Neutrophil extracellular trap formation (Fig. 5C). As a result, the molecular subtypes exhibited differences in functional activities and metabolic pathways.

Molecular subtype tumor mutations

Somatic gene mutations are crucial drivers of cancer pathogenesis. Therefore, we analyzed the differences in somatic mutation frequencies between the two subtypes. Utilizing the MafTools R package, we conducted an analysis and visualization of the mutation data between the molecular subtypes. The top 20 mutated genes and their frequencies differed between the subtypes, and the mutation types were predominantly Missense Mutations, with C > A and C > T being the most frequent SNV mutations (SNV Class). The stacked bar plot depicted the top ten mutated genes in each subtype. For cluster-1, the top ten mutated genes were TTN, MUC16, CSMD3, RYR2, TP53, LRP1B, USH2A, FLG, ZFHX4, and KRAS. In cluster-2, they were TTN, CSMD3, MUC16, RYR2, LRP1B, USH2A, ZFHX4, TP53, XIRP2, and SPTA1. Additionally, cluster-2 exhibited higher sample mutation rates and gene mutation rates compared to cluster-1 (Fig. 6A-D). Overall, this suggested an association between molecular subtypes and gene mutations.

Targeted small molecules for molecular subtypes

Using the cMAP database, we predicted small molecule compounds targeted for LUAD. The prediction was based on the Score. The molecule compounds with the lowest 10 scores represented the predicted drugs. Utilizing the DEGs between the molecular subtypes, we identified teniposide, RO-28-1675, phloretin, pyrvinium-pamoate, olaparib, aminopurvalanol-a, purvalanol-a, JNJ-26854165, and WZ-4-145 as the ten most relevant drugs. These compounds could potentially serve as prospective candidate drugs for LUAD patients (Table 1).

Discussion

In recent years, researchers have proposed various molecular classifications of LUAD tumors, including subtypes based on immune infiltration, MRGs, proteomics, non-coding RNA, and epigenetic modifications (Borczuk 2016; Chalela et al. 2017; Huang et al. 2023). These classifications have contributed to the advancement of LC diagnosis and treatment, offering significant benefits to patients (Cooper et al. 2013; Sun et al. 2020; Huang et al. 2023). Additionally, studies have highlighted the tight connection between LC development and metabolism as well as immunity (Bamji-Stocke et al. 2018). However, there has been

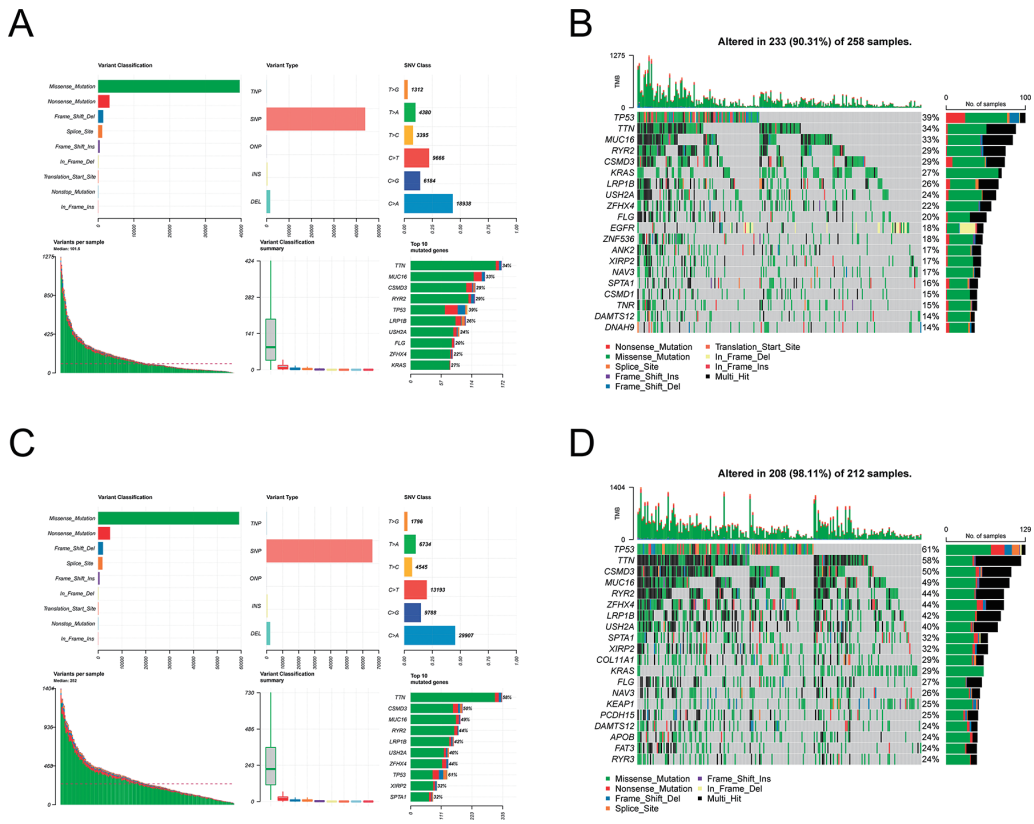

Fig. 6. Analysis of molecular subtype tumor mutations.
(A) Mutation information in cluster-1; (B) The waterfall map was used to show the top 20 mutant genes and their distribution in cluster-1 group; (C) Mutation information in cluster-2; (D) The waterfall map was used to show the top 20 mutant genes and their distribution in cluster-2 group.

Table 1. Small molecules of LUAD predicted by DEGs of molecular subtypes.

Score	Type	ID	Name	Description
−100	cp	BRD-A35588707	teniposide	Topoisomerase inhibitor
−100	cp	BRD-K21672174	RO-28-1675	Glucokinase activator
−100	cp	BRD-K05653692	DL-PDMP	Glucosyltransferase inhibitor
−100	cp	BRD-K15563106	phloretin	Sodium/glucose cotransporter inhibitor
−99.96	cp	BRD-M86331534	pyrvinium-pamoate	AKT inhibitor
−99.96	cp	BRD-K02113016	olaparib	PARP inhibitor
−99.96	cp	BRD-K07762753	aminopurvalanol-a	Tyrosine kinase inhibitor
−99.96	cp	BRD-K50836978	purvalanol-a	CDK inhibitor
−99.93	cp	BRD-K83837640	JNJ-26854165	HDAC inhibitor
−99.93	cp	BRD-U25771771	WZ-4-145	EGFR inhibitor

limited research simultaneously addressing the closely intertwined fields of metabolism and immunity that are critical to cancer pathogenesis. Recently, Guo et al. (2022) utilized bioinformatics analysis to uncover the crucial roles of IMRGs in hepatocellular carcinoma tumorigenesis and progression. Thus, building upon the current understanding of LUAD, we conducted a study focusing on IMRGs in the context of LUAD. Specifically, based on the expression profiles of IMRGs, we categorized LUAD samples into two distinct classes. We comprehensively described the molecular characteristics of these subtypes by evaluating immune cell infiltration, immunotherapy response, PPI and enrichment analysis, somatic mutations, and prediction of targeted small molecule drugs. The outcomes of this study enhanced our comprehension of LUAD's molecular features and held the potential to improve personalized and precise clinical management for LUAD.

Dividing LUAD patients into cluster-1 and cluster-2 groups, we observed that patients in the cluster-1 group exhibited longer survival and a richer infiltration of immune cells, such as aDCs, B cells, DCs, iDCs, Macrophages, Mast cells, Neutrophils, pDCs, T helper cells, TIL, and

Treg. This suggested a close association between cluster-1 patients and lymphocytic infiltration in the tumor milieu. Previous research has demonstrated that high-density tumor-infiltrating lymphocytes can suppress tumor progression (Park et al. 2022), particularly in patients undergoing ICI therapy (Lopez de Rodas et al. 2022). The IPS and TIDE scores are used to predict patients' response to immunotherapy by assessing the potential for tumor immune escape (Wang et al. 2023). In our study, we found that cluster-1 patients had higher IPS and lower TIDE scores compared to cluster-2 patients, indicating that cluster-1 patients might derive more benefit from ICI treatment. This further supported the notion of a favorable immunotherapy response in cluster-1 patients.

Regarding gene mutations, the favorable prognosis cluster-1 and the unfavorable prognosis cluster-2 exhibited low and high frequencies of gene mutations, respectively. Gene mutations in cancer cells provide a mechanism for the overexpression of oncogenic driver genes or the suppression of anti-cancer genes (Roepman et al. 2009). Several common tumor-associated genes, including TP53 and KRAS, show lower expression in cluster-1. TP53 is a human tumor suppressor gene, and its variants are associated with LC risk, prognosis, and somatic mutations in lung tumors (Mechanic et al. 2007). Cluster-2 demonstrates elevated expression of TP53 mutations, thus indicating higher risk and adverse prognosis. Furthermore, reports suggested that LC with dual mutations in TP53 and other genes may have a poorer prognosis (La Fleur et al. 2019). We found that the expression of genes like KRAS, TTN, CSMD3, and RYR2 was lower in cluster-1 compared to cluster-2. Therefore, we speculated that the combination of TP53 gene mutations with other gene mutations might contribute to adverse prognosis. Additionally, we predicted therapeutic small molecule compounds for LUAD, including Teniposide, phloretin, and pyrvinium-pamoate. Teniposide has been shown to enhance the efficacy of programmed cell death protein-1 antibody therapy (Li et al. 2022). Phloretin exhibits activity in regulating metabolic homeostasis and anti-inflammation (Mao et al. 2022). Pyrvinium-pamoate can block STAT3 synthesis in KRAS-mutated LC, leading to cell death. Thus, the predicted compounds held potential for preventing LUAD progression.

In conclusion, our work shed light on the molecular characteristics of LUAD and might contribute to the refinement of immunotherapy approaches for LUAD. However, limitations existed. Firstly, due to the lack of clinical information regarding ICI therapy in the TCGA database, we could only assess the potential responsiveness to ICI therapy based on IPS and TIDE analyses. Secondly, the correlation between immune-related features and ICI therapy sensitivity, as well as potential mechanisms of metabolism reprogramming, remain to be further validated through *in vitro* basic research and *in vivo* clinical studies. Finally, the therapeutic efficacy of the small molecule drugs predicted from the cMAP database for LUAD is unknown in the clinical context and requires validation through subsequent animal experiments and clinical trials.

Author Contributions

Conceptualization: Mengna Wang and Hongbo Xia; Data curation: Mengna Wang; Formal Analysis: Hongbo Xia; Writing: Mengna Wang; Supervision: Hongbo Xia

Conflict of Interest

The authors declare no conflict of interest.

References

Bader, J.E., Voss, K. & Rathmell, J.C. (2020) Targeting Metabolism to Improve the Tumor Microenvironment for Cancer Immunotherapy. *Mol. Cell*, **78**, 1019-1033.

Bamji-Stocke, S., van Berkel, V., Miller, D.M. & Frieboes, H.B. (2018) A review of metabolism-associated biomarkers in lung cancer diagnosis and treatment. *Metabolomics*, **14**, 81.

Bhattacharya, S., Andorf, S., Gomes, L., Dunn, P., Schaefer, H., Pontius, J., Berger, P., Desborough, V., Smith, T., Campbell, J., Thomson, E., Monteiro, R., Guimaraes, P., Walters, B., Wiser, J., et al. (2014) ImmPort: disseminating data to the public for the future of immunology. *Immunol. Res.*, **58**, 234-239.

Blandin Knight, S., Crosbie, P.A., Balata, H., Chudziak, J., Hussell, T. & Dive, C. (2017) Progress and prospects of early detection in lung cancer. *Open Biol.*, **7**, 170070.

Borczuk, A.C. (2016) Prognostic considerations of the new World Health Organization classification of lung adenocarcinoma. *Eur. Respir. Rev.*, **25**, 364-371.

Cancer Genome Atlas Research, Network (2014) Comprehensive molecular profiling of lung adenocarcinoma. *Nature*, **511**, 543-550.

Chalela, R., Curull, V., Enriquez, C., Pijuan, L., Bellosillo, B. & Gea, J. (2017) Lung adenocarcinoma: from molecular basis to genome-guided therapy and immunotherapy. *J. Thorac. Dis.*, **9**, 2142-2158.

Choi, H. & Na, K.J. (2018) Integrative analysis of imaging and transcriptomic data of the immune landscape associated with tumor metabolism in lung adenocarcinoma: Clinical and prognostic implications. *Theranostics*, **8**, 1956-1965.

Cooper, W.A., Lam, D.C., O'Toole, S.A. & Minna, J.D. (2013) Molecular biology of lung cancer. *J. Thorac. Dis.*, **5** Suppl 5, S479-490.

Cui, S., Zhang, M., Bai, S., Bi, Y., Cong, S., Jin, S., Li, S., He, H. & Zhang, J. (2023) Development of Prognostic Features of Hepatocellular Carcinoma Based on Metabolic Gene Classification and Immune and Oxidative Stress Characteristic Analysis. *Oxid. Med. Cell. Longev.*, **2023**, 1847700.

Guo, Y., Yang, J., Gao, H., Tian, X., Zhang, X. & Kan, Q. (2022) Development and Verification of a Combined Immune- and Metabolism-Related Prognostic Signature for Hepatocellular Carcinoma. *Front. Immunol.*, **13**, 927635.

Hänzelmann, S., Castelo, R. & Guinney, J. (2013) GSVA: gene set variation analysis for microarray and RNA-seq data. *BMC Bioinformatics*, **14**, 7.

Huang, X., Zhang, F., Lin, J., Lin, S., Shen, G., Chen, X. & Chen, W. (2023) Systematically analyzed molecular characteristics of lung adenocarcinoma using metabolism-related genes classification. *Genet. Mol. Biol.*, **45**, e20220121.

Inamura, K. (2018) Clinicopathological Characteristics and Mutations Driving Development of Early Lung Adenocarcinoma: Tumor Initiation and Progression. *Int. J. Mol. Sci.*, **19**, 1259.

Kashima, J., Kitadai, R. & Okuma, Y. (2019) Molecular and Morphological Profiling of Lung Cancer: A Foundation for "Next-Generation" Pathologists and Oncologists. *Cancers* (*Basel*), **11**, 599.

La Fleur, L., Falk-Sorqvist, E., Smeds, P., Berglund, A., Sundstrom, M., Mattsson, J.S., Branden, E., Koyi, H., Isaksson, J., Brunnstrom, H., Nilsson, M., Micke, P., Moens, L. & Botling, J. (2019) Mutation patterns in a population-based non-small cell lung cancer cohort and prognostic impact of concomitant mutations in KRAS and TP53 or STK11. *Lung Cancer*, **130**, 50-58.

Li, K., Gong, Y., Qiu, D., Tang, H., Zhang, J., Yuan, Z., Huang, Y., Qin, Y., Ye, L. & Yang, Y. (2022) Hyperbaric oxygen facilitates teniposide-induced cGAS-STING activation to enhance the antitumor efficacy of PD-1 antibody in HCC. *J. Immunother. Cancer*, **10**, e004006.

Li, X., Wenes, M., Romero, P., Huang, S.C., Fendt, S.M. & Ho, P.C. (2019) Navigating metabolic pathways to enhance antitumour immunity and immunotherapy. *Nat. Rev. Clin. Oncol.*, **16**, 425-441.

Liu, B., Wang, C., Fang, Z., Bai, J., Qian, Y., Ma, Y., Ruan, X., Yan, S., Li, S., Wang, Y., Dong, B., Yang, X., Li, M., Xia, X., Qu, H., et al. (2022) Single-cell RNA sequencing reveals the cellular and molecular changes that contribute to the progression of lung adenocarcinoma. *Front. Cell Dev. Biol.*, **10**, 927300.

Lopez de Rodas, M., Nagineni, V., Ravi, A., Datar, I.J., Mino-Kenudson, M., Corredor, G., Barrera, C., Behlman, L., Rimm, D.L., Herbst, R.S., Madabhushi, A., Riess, J.W., Velcheti, V., Hellmann, M.D., Gainor, J., et al. (2022) Role of tumor infiltrating lymphocytes and spatial immune heterogeneity in sensitivity to PD-1 axis blockers in non-small cell lung cancer. *J. Immunother. Cancer*, **10**, e004440.

Mao, W., Fan, Y., Wang, X., Feng, G., You, Y., Li, H., Chen, Y., Yang, J., Weng, H. & Shen, X. (2022) Phloretin ameliorates diabetes-induced endothelial injury through AMPK-dependent anti-EndMT pathway. *Pharmacol. Res.*, **179**, 106205.

Martinez-Reyes, I. & Chandel, N.S. (2021) Cancer metabolism: looking forward. *Nat. Rev. Cancer*, **21**, 669-680.

Mayakonda, A., Lin, D.C., Assenov, Y., Plass, C. & Koeffler, H.P. (2018) Maftools: efficient and comprehensive analysis of somatic variants in cancer. *Genome Res.*, **28**, 1747-1756.

Mechanic, L.E., Bowman, E.D., Welsh, J.A., Khan, M.A., Hagiwara, N., Enewold, L., Shields, P.G., Burdette, L., Chanock, S. & Harris, C.C. (2007) Common genetic variation in TP53 is associated with lung cancer risk and prognosis in African Americans and somatic mutations in lung tumors. *Cancer Epidemiol. Biomarkers Prev.*, **16**, 214-222.

Newman, A.M., Liu, C.L., Green, M.R., Gentles, A.J., Feng, W., Xu, Y., Hoang, C.D., Diehn, M. & Alizadeh, A.A. (2015) Robust enumeration of cell subsets from tissue expression profiles. *Nat. Methods*, **12**, 453-457.

Nooreldeen, R. & Bach, H. (2021) Current and Future Development in Lung Cancer Diagnosis. *Int. J. Mol. Sci.*, **22**, 8661.

Park, S., Ock, C.Y., Kim, H., Pereira, S., Park, S., Ma, M., Choi, S., Kim, S., Shin, S., Aum, B.J., Paeng, K., Yoo, D., Cha, H., Park, S., Suh, K.J., et al. (2022) Artificial Intelligence-Powered Spatial Analysis of Tumor-Infiltrating Lymphocytes as Complementary Biomarker for Immune Checkpoint Inhibition in Non-Small-Cell Lung Cancer. *J. Clin. Oncol.*, **40**, 1916-1928.

Robinson, M.D., McCarthy, D.J. & Smyth, G.K. (2010) edgeR: a Bioconductor package for differential expression analysis of digital gene expression data. *Bioinformatics*, **26**, 139-140.

Roepman, P., Jassem, J., Smit, E.F., Muley, T., Niklinski, J., van de Velde, T., Witteveen, A.T., Rzyman, W., Floore, A., Burgers, S., Giaccone, G., Meister, M., Dienemann, H., Skrzypski, M., Kozlowski, M., et al. (2009) An immune response enriched 72-gene prognostic profile for early-stage non-small-cell lung cancer. *Clin. Cancer Res.*, **15**, 284-290.

Seguin, L., Durandy, M. & Feral, C.C. (2022) Lung Adenocarcinoma Tumor Origin: A Guide for Personalized Medicine. *Cancers* (*Basel*), **14**, 1759.

Socinski, M.A., Obasaju, C., Gandara, D., Hirsch, F.R., Bonomi, P., Bunn, P., Kim, E.S., Langer, C.J., Natale, R.B., Novello, S., Paz-Ares, L., Perol, M., Reck, M., Ramalingam, S.S., Reynolds, C.H., et al. (2016) Clinicopathologic Features of Advanced Squamous NSCLC. *J. Thorac. Oncol.*, **11**, 1411-1422.

Sun, J., Zhang, Z., Bao, S., Yan, C., Hou, P., Wu, N., Su, J., Xu, L. & Zhou, M. (2020) Identification of tumor immune infiltration-associated lncRNAs for improving prognosis and immunotherapy response of patients with non-small cell lung cancer. *J. Immunother. Cancer*, **8**, e000110.

Sung, H., Ferlay, J., Siegel, R.L., Laversanne, M., Soerjomataram, I., Jemal, A. & Bray, F. (2021) Global Cancer Statistics 2020: GLOBOCAN Estimates of Incidence and Mortality Worldwide for 36 Cancers in 185 Countries. *CA Cancer J. Clin.*, **71**, 209-249.

Wang, T., Guo, K., Zhang, D., Wang, H., Yin, J., Cui, H. & Wu, W. (2023) Disulfidptosis classification of hepatocellular carcinoma reveals correlation with clinical prognosis and immune profile. *Int. Immunopharmacol.*, **120**, 110368.

Wilkerson, M.D. & Hayes, D.N. (2010) ConsensusClusterPlus: a class discovery tool with confidence assessments and item tracking. *Bioinformatics*, **26**, 1572-1573.

Xia, L., Oyang, L., Lin, J., Tan, S., Han, Y., Wu, N., Yi, P., Tang, L., Pan, Q., Rao, S., Liang, J., Tang, Y., Su, M., Luo, X., Yang, Y., et al. (2021) The cancer metabolic reprogramming and immune response. *Mol. Cancer*, **20**, 28.

Yang, K., Dinasarapu, A.R., Reis, E.S., Deangelis, R.A., Ricklin, D., Subramaniam, S. & Lambris, J.D. (2013) CMAP: Complement Map Database. *Bioinformatics*, **29**, 1832-1833.

Yoshihara, K., Shahmoradgoli, M., Martinez, E., Vegesna, R., Kim, H., Torres-Garcia, W., Trevino, V., Shen, H., Laird, P.W., Levine, D.A., Carter, S.L., Getz, G., Stemke-Hale, K., Mills, G.B. & Verhaak, R.G. (2013) Inferring tumour purity and stromal and immune cell admixture from expression data. *Nat. Commun.*, **4**, 2612.

Yu, G., Wang, L.G., Han, Y. & He, Q.Y. (2012) clusterProfiler: an R package for comparing biological themes among gene clusters. *OMICS*, **16**, 284-287.

Zeng, W., Wang, J., Yang, J., Chen, Z., Cui, Y., Li, Q., Luo, G., Ding, H., Ju, S., Li, B., Chen, J., Xie, Y., Tong, X., Liu, M. & Zhao, J. (2023) Identification of immune activation-related gene signature for predicting prognosis and immunotherapy efficacy in lung adenocarcinoma. *Front. Immunol.*, **14**, 1217590.

Supplementary Files

Please find supplementary file(s);
https://doi.org/10.1620/tjem.2024.J086